Mapping global fisheries climate risks to guide sustainable marine management

Matthew P. Faith[1,2], Angus Atkinson[3*], Ryan F. Heneghan[4], Clare Ostle[5], Jose A. Fernandes-Salvador[6], Murray S. A. Thompson[7], Camila Serra-Pompei[8], Yuri Artioli[3], Katrin Schmidt[9], Sian Rees[1], Matthew Holland[1], Abigail McQuatters-Gollop[1]

[1]School of Biological and Marine Sciences, University of Plymouth, Drake Circus, Plymouth, PL4 8AA, UK.
[2]The Alan Turing Institute,British Library, 96 Euston Road, London, NW1 2DB, UK.
[3]Plymouth Marine Laboratory, Prospect Place, The Hoe, Plymouth, PL1 3DH UK.
[4]School of Environment and Science, Griffith University, Nathan, 4111, QLD, Australia.
[5]The Marine Biological Association (MBA), The Laboratory, Citadell Hill, Plymouth, PL1 2PB, UK.
[6]AZTI Marine Research, Basque Research and Technology Alliance (BRTA), Txatxarramendi Ugartea z/g, Sukarrieta, 48395, Spain.
[7]Centre for Environment, Fisheries and Aquaculture Science (Cefas), Lowestoft Laboratory, Pakefield Road, Lowestoft, NR33 0HT, UK.
[8]National Institute for Aquatic Resources, Technical University of Denmark, 2800 Kgs. Lyngby, Denmark.
[9]School of Geography, Earth and Environmental Sciences, University of Plymouth, Drake Circus, Plymouth, PL4 8AA, UK.

*Corresponding author(s). E-mail(s): aat@pml.ac.uk;

Abstract

Ocean warming is projected to threaten fisheries, but the extent varies greatly between models due to a poor understanding of how complex food webs respond to change. Likewise, inequalities in socioeconomic dependence on fisheries and

uneven distributions of global fishing effort make it unclear how the distribution of fisheries declines could translate into socioeconomic impacts. Here we developed a quantitative IPCC tripartite risk mapping approach, combining hazard (projected pelagic fish decline), exposure (present day pelagic fishing intensity), and vulnerability (national dependence on fisheries) to generate global maps of pelagic fishery climate risk. Using a direct, empirical method of projecting fish trends based on plankton size-spectra, our risk mapping approach identifies fishing grounds across Southeast Asia, western seaboards of Africa and South America and adjacent islands at highest risk. We project substantial declines (∼20%) in supportable fish biomass by the end of the century under a high emission scenario, which could be reduced (to ∼10%) by strong global climate mitigation measures. With climate mitigation being the only clear route to curbing declines in fisheries carrying capacity, our approach guides the spatial prioritisation of broader mitigation measures which reduce other human pressures on fish stocks, including effort control and the development of protected areas which support essential fish habitats. High-risk regions extend into Areas Beyond National Jurisdiction, highlighting the potential for the upcoming High Seas Treaty to introduce fisheries management measures which serve to offset a substantial socioeconomic risk under climate change.

1 Main text

Pelagic fish provide valuable ecosystem services, including contributing to the food and economic security of billions of people through capture fisheries [1]. Global fish stocks are under threat from multiple pressures, including over-fishing, eutrophication, habitat destruction, and climate change effects [2, 3]. Long-term ocean warming is a key climate effect impacting fisheries, as widescale warming-induced decreases in marine phytoplankton biomass are projected to reduce the supportable biomass of fish [4–8]. Rising sea surface temperatures have already led to increased stratification and surface nutrient-depletion, causing ocean-scale declines in phytoplankton biomass [9–11], a trend which is set to continue with future climate change [12]. Nutrient depletion is associated with overall decreases in phytoplankton biomass [9] and shifts in the size structure of phytoplankton communities, as picophytoplankton can outcompete larger diatoms and dinoflagellates in nutrient-poor environments [13]. These climate-driven ecological changes in phytoplankton communities are associated with reduced food web efficiency and ultimately impact the supportable biomass of higher trophic levels, including fish [8]. Climate-driven declines in fish biomass are a societal threat, putting at risk the food and economic security of the communities who rely on fisheries.

To help assess the magnitude of future climate-driven fisheries declines, a range of process-based, mechanistic marine ecosystem models have been developed to project climate-driven changes in marine biomass at different trophic levels [14–16]. However, a lack of consensus on the physiological impacts of ocean warming and the best approach to resolve linkages between lower and higher trophic levels have resulted in

large discrepancies between the outputs of different ecosystem models [17, 18]. The slopes of Normalised Biomass Size Spectra (hereafter "size spectrum slopes") provide an empirical alternative to widely-used process-based modelling of climate change impacts on fish biomass [8].

Size spectrum slopes capture a key property of ecosystems - the relative abundance of small and large organisms. Thus, steeper negative size spectrum slopes (increasingly fewer large versus small organisms) signify, on average and over large spatial scales, reduced efficiency of energy transfer through the food web [19]. Warmer temperatures may result in steeper size spectrum slopes, for example through directly reducing the transfer efficiency from one trophic level to the next, or indirectly by impacting primary producers, as reduced nutrient levels favour smaller, less-nutritious primary producers [13, 20]. However, several authors have now found evidence that indirect effects via shifts in food resources can be stronger than direct effects of temperature on consumer physiology [8, 21]. While empirical size spectrum slope approaches have only recently been developed in a climate change context [22–24], using the macro-scale relationships of observed size spectrum slopes with temperature and chlorophyll concentration enables projections of climate change impacts on fish biomass [8, 19, 24]. Size spectrum-based projections are likely to signal impacts to a range of fish functional groups but are intuitively linked most strongly with pelagic fish, with more direct trophic transfer from phytoplankton to fish. Atkinson et al. [8] found chlorophyll-a concentration to be a good predictor of size spectrum slopes, with declines in chlorophyll-a translating to a steepening of the size spectrum slopes from phytoplankton to fish. Projected future decreases in chlorophyll-a and phytoplankton biomass can thus be used to estimate changes in the supportable biomass of fish available to pelagic fisheries [8].

To target effective climate adaptation and mitigation measures and ultimately reduce the negative societal impacts from climate change effects, the Intergovernmental Panel on Climate Change (IPCC) assess risks of 'losses and damages' [25]. Losses and damages can be economic (e.g., financial losses associated with infrastructure damage from increased flooding) or non-economic (e.g., harms to human health from extreme heat). To reduce future climate effects, and subsequent risks of losses and damages, mitigation measures aim to reduce greenhouse gas emissions and ultimately curb continuing trends of global warming. However, overall climate risks are also driven by patterns of societal exposure and vulnerability to climate effects [26]. For example, many low-lying Small Island Developing States are particularly exposed to the effects of sea level rises and thus face disproportionate risks of losses and damages [27]. Adaptation measures therefore aim to reduce the exposure or vulnerability of communities to climate effects, thus reducing the risks of losses and damages (e.g., constructing coastal defences to reduce the risks of damages from coastal flooding with ongoing sea level rise). Climate risk assessments have also recently expanded to include the losses and damages from the ecosystem service losses driven by climate effects [25, 28, 29]. In the context of IPCC risk-based approaches, the potential for societal losses and damages resulting from climate-driven fisheries declines can therefore be considered

a climate risk (hereafter referred to as 'fisheries climate risk'; Figure 1). Considering fisheries climate risks through this tripartite IPCC approach (Figure 1) thus combines hazard, exposure and vulnerability into a single risk factor.

Figure 1 - Applying climate risk assessment approaches from the International Panel on Climate Change (IPCC) to fisheries.

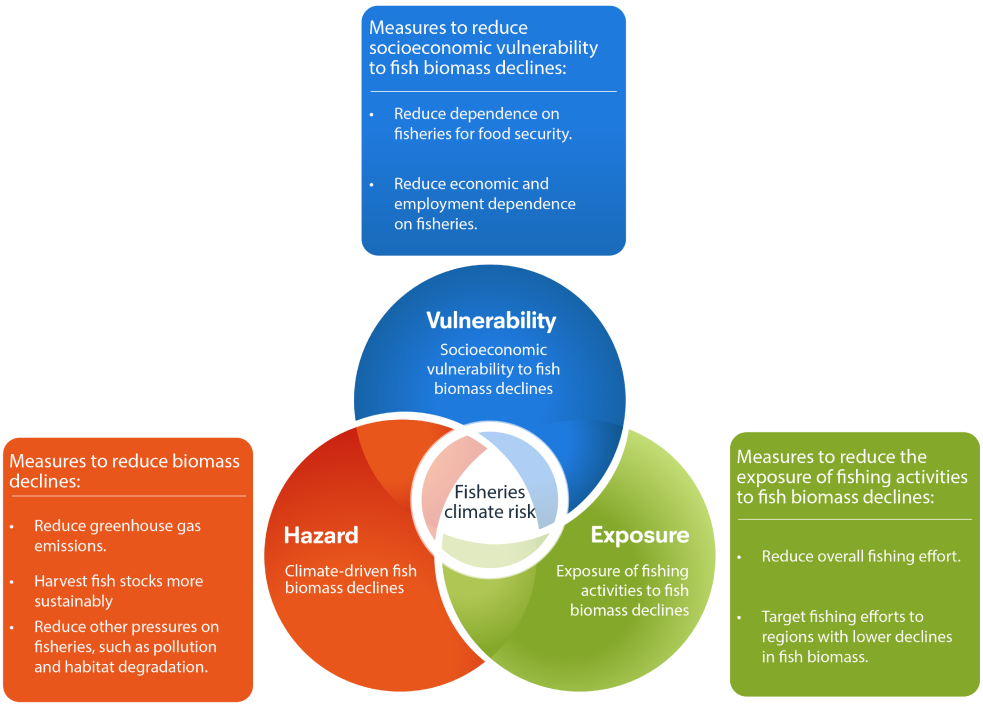

Fisheries climate risk captures the potential for societal losses and damages as fish biomass declines with continued ocean warming. This figure was adapted from Figure TS.4 in the Technical Summary of the IPCC Special Report on the Ocean and Cryosphere in a Changing Climate (IPCC, 2019).

Understanding the magnitude and spatial distribution of projected fisheries declines with climate change provides valuable evidence to decision-makers of the potential impacts on regional fish landings [15]. Previous research has identified the disproportionate impact of projected fish biomass declines within the Exclusive Economic Zones (EEZs) of fisheries-dependent nations [30, 31], highlighting the importance of considering regional vulnerabilities when assessing fisheries climate risks. National-level fisheries climate impact assessments [15, 30, 32] are therefore vital for guiding efforts to reduce national vulnerabilities to fisheries climate risks (Figure 1). However, nearly a quarter (23%) of fish landings are in regions beyond

national jurisdiction (in the High Seas) or in foreign territories [33], and even the fishing patterns within EEZs are not spatially uniform. While fishing patterns are likely to change in the future [34], understanding the co-location of fish biomass declines with present day fishing activities could reveal the exposure of fishing activities to projected biomass declines. By using global fishing patterns to guide our risk assessment, we identify fishing grounds that pose the highest risks for socioeconomic losses and damages under climate change and thus will require more conservative fisheries management, or where risk is lower and offer opportunities for future fisheries. Such information will be critical to help ensure sustainable fisheries into the future by identifying priority regions where the risks of a declining fisheries carrying capacity must be mitigated to avoid socioeconomic losses and damages (Figure 1).

Here, we make the first climate risk assessment of global pelagic capture fisheries using current patterns of fishing. We combine Earth System Model outputs and size spectrum slopes to project the future supportable biomass of fish. To increase trust in our projections, we compare historical changes in zooplankton biomass (the nearest trophic level below fish with high quality long-term time-series) to projections of future fish biomass. We then couple our fish biomass projections with present day fishing patterns as a novel approach to identifying the pelagic fishing grounds set to be most exposed to projected fish biomass declines. Using a metric of fisheries socioeconomic dependence by country, we further assess the relative importance of global fishing grounds to the food and economic security of the nations who fish there. Finally, by combining our fish biomass projections (hazard) with current day fishing patterns (exposure) and fisheries socioeconomic metrics (vulnerability), we assess the overall climate risks to present-day pelagic fishing grounds. Our tripartite IPCC approach (Figure 1) provides a valuable tool for identifying fishing grounds at the highest risk under a changing climate, where management measures which reduce other pressures on fish stocks should be prioritised.

2 Results

2.1 Projected declines of global fish biomass

Steepening size spectrum slopes, coupled with decreasing phytoplankton biomass across much of the marine environment, are projected to drive substantial decreases in the fish biomass that can be supported (Figures 2a-d; see SI Figure 4 for projected size spectra changes and SI Figure 2 for phytoplankton biomass changes). Even under a low emission scenario (SSP 1-2.6), notable declines of supportable fish biomass are projected by 2040-2049 (relative to 1990-1999), with a global mean decrease of 8.9% (CI 6.8 – 10.8%; Figure 2a). Under a high emission scenario (SSP 5-8.5), 2040-2049 declines in supportable fish biomass (Figure 2b) are projected to be similar to low emission declines, with a global mean decrease of 9.7% (CI 7.3 – 11.9%). By the end of the century (2090-2099) fish biomass declines are slightly dampened to a global mean decrease of 8.5% (CI 6.7 – 10.2%) under a low emissions scenario (Figure 2c). However, by the end of the century, a high emissions scenario is projected to result in mean average supportable biomass declines of 20.1% (CI 15.5 – 23.9%; Figure 2d).

Figure 2 - The effects of continued ocean warming on phytoplankton are projected to reduce the supportable biomass of fish.

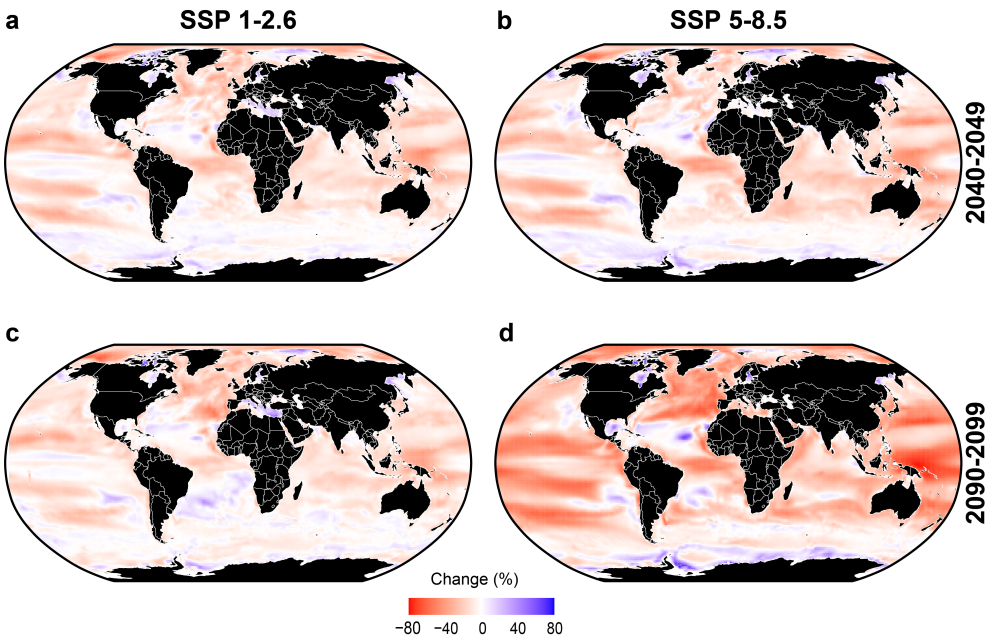

Percentage changes in total supportable fish biomass (g C m^{-2}) between 1990-1999 and 2040-2049 under **a**). SSP 1-2.6 and **b**). SSP 5-8.5; between 1990-1999 and 2090-2099 under **c**). SSP 1-2.6 and **d**). SSP 5-8.5.

2.2 Fisheries risk assessment

We undertook a climate risk assessment (Figure 1) of global fisheries targeting pelagic species, by combining our projections of fish biomass declines (Figure 2, 3a), with current pelagic fishing patterns (Figure 3b), and an assessment of the socioeconomic importance of fishing grounds to the nations who fish there (Figure 3c). Fishing activities targeting pelagic fish (full size range; Figure 3b) contributed to 36% of global fishing effort between 2014-2017. There was a great degree of overlap between areas with large projected declines in fish biomass (Figure 3a) and those with high present-day pelagic fishing activity (Figure 3b), such as Southeast Asia, the Northeast Atlantic and the southern coastline of South America (see SI Figure 6 for fisheries hazard-exposure metrics). Small Island Developing States, such as the Federated States of Micronesia and Tuvalu, alongside North Atlantic fishing nations, such as Greenland, Iceland and the Faroes, were found to be among the most dependent on fisheries and thus relatively more vulnerable to fish biomass declines (see SI Table 1 for full list of vulnerability indicators). Inequalities in national fisheries vulnerability translated into

hotspots in the ocean where fishing grounds are relatively more depended upon by the nations who fish there (Figure 3c), particularly across Southeast Asia, the South Pacific and the northern edge of the Atlantic Ocean, alongside hotspots in South Asia and the coasts of Africa.

Figure 3 - Climate risk maps to fisheries based on combining hazard, exposure and vulnerability shows hotspots near fisheries-dependent nations.

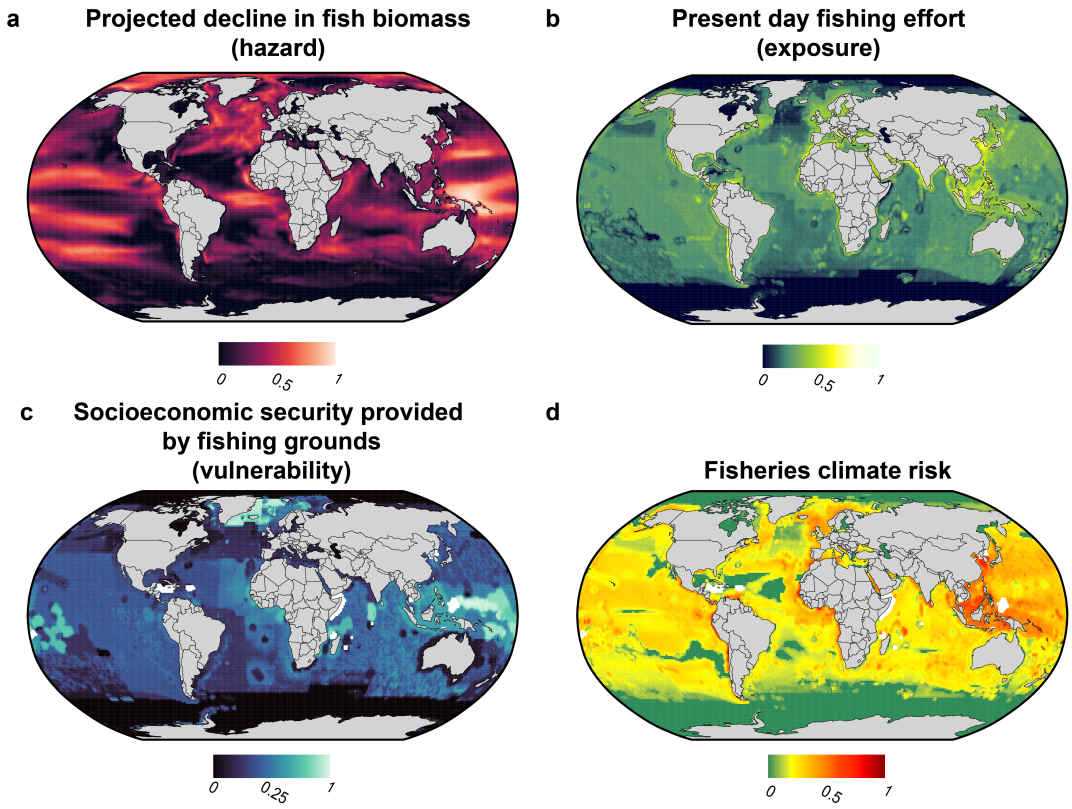

a). Projected trend in supportable fish biomass decline between 1990-1999 and 2090-2099 under SSP 5-8.5, derived from size spectra model; **b**). mean total annual pelagic nominal fishing effort between 2014-2017, processed from Rousseau *et al.* (2024); **c**). mean average fishing dependency metric, updated from Blanchard *et al.* (2017), weighted by total annual pelagic nominal fishing effort by country from Rousseau *et al.* (2024) (see methods); **d**). overall climate risk, calculated as the product of **a**, **b**, and **c**. All metrics (**a**, **b**, **c**, and **d**) were scaled between 0 and 1 without transformation; to aid presentation, **a** and **d** were transformed ($y = x^{0.15}$) and rescaled between 0 and 1. Missing data is shown in white.

Our resultant pelagic fishing ground tripartite climate risk map (Figure 3d) addresses the co-location of projected declines in fish biomass with regions of intense pelagic fishing activities and high socioeconomic dependence on fisheries. We found that with continued ocean warming, socioeconomic losses and damages were most likely to be caused by impacts to fishing grounds across Southeast Asia and the western Pacific, and thus these regions were assessed as high risk. Other high-risk regions can be seen along the west coast of Africa, and the western coastline of South and Central America. Medium-risk regions were identified with combined high-intensity fishing and substantial projected fish biomass declines but lower socioeconomic fisheries dependence, such as the coasts of the UK and Canada, while other medium-risk regions are highly depended upon for socioeconomic security but are projected to see relatively moderate declines in fish biomass, such as the Maldives.

2.3 Inter-validation of projections in the Northeast Atlantic

To provide an independent approach to validate our projections qualitatively, we examined the Northeast Atlantic region in more detail. This region was selected due to substantial projected fish biomass declines (Figure 2), intensive fishing activities (Figure 4d), and long-term zooplankton abundance time series data provided by the Continuous Plankton Recorder (CPR) Survey [35]. The Northeast Atlantic region has warmed over the past 50 years [36], and if our projections that future warming will lead to declines in fish are valid, we should expect to see some evidence for a fish decline over the last half century of warming. While fish catches per unit effort have declined [37], fish indices are problematic to interpret due to the complex interactions of climate change and overfishing [38]. The nearest trophic level to fish with sufficiently long temporal-spatial time-series is zooplankton, which are routinely collected by the CPR Survey. Here we have calculated, for the first time, long-term trends in total zooplankton biomass across the NE Atlantic (Figure 4a). These trends indicate a general decline of total zooplankton biomass between 1958 and 2021, with the decline being strongest in oceanic areas, in common with the areas of greatest projected fish decline. However, the key point is that the biomass of zooplankton, which consume phytoplankton and are consumed by fish, has declined during the last 60 years of warming, increasing confidence in our projection that the supportable biomass of fish will continue to decline under future warming.

Figure 4 - Projections of declining fish biomass across the NE Atlantic are supported by higher-resolution modelling and by the reductions in zooplankton biomass observed over the last 60 years of warming.

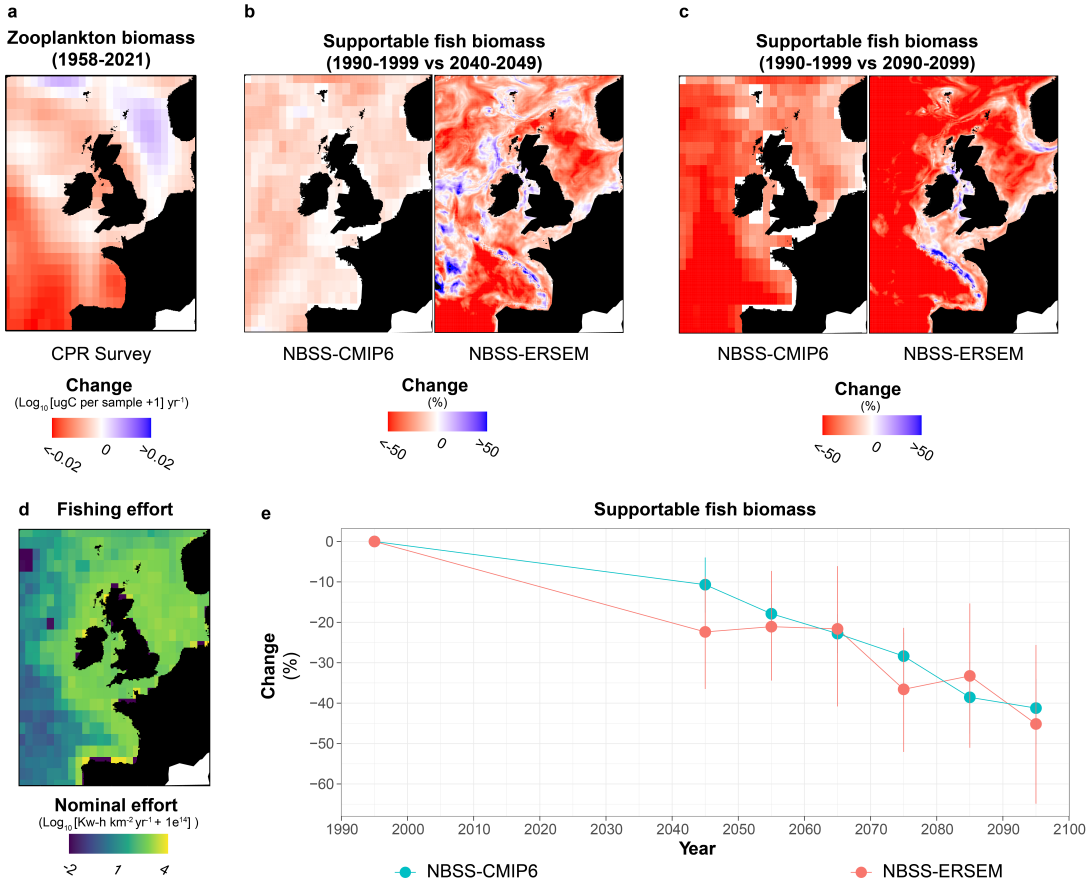

a). Change in zooplankton biomass from observations over the last 60 years based on the Continuous Plankton Recorder (CPR) survey. These are compared on the same scale with projected changes in supportable fish biomass by **b).** 2040-2049 and **c).** by 2090-2099. Projections are based on NEMO-ERSEM and CMIP6 Earth System model outputs of phytoplankton changes relative to 1990-1999 under a high emissions scenario (Shared Socioeconomic Pathway 5-8.5 for CMIP6 and Representative Concentration Pathway 8.5 for NEMO-ERSEM), from which our size spectrum slope method was used to estimate changes in fish biomass. **d).** Mean total annual pelagic nominal fishing effort between 2014-2017, processed from Rousseau *et al.* (2024). **e).** Projected changes in total values over time across the whole map domain (see Methods). Decadal averages were plotted as mid-decade (e.g., 1990-1999 is plotted as 1995).

Changes in phytoplankton used as inputs to our size spectrum-based projections are outputs from Earth System Models, which are known to have issues in localised shelf environments [32]. Therefore, to provide a further test of our projections, we compared outputs based on the NEMO-ERSEM modelling system [39] to the Earth

System Models used in CMIP6, which were used for global projections (Figure 2). NEMO-ERSEM projections are made over much finer scales in comparison with CMIP6 models and include a greater range of physical and biological processes. Phytoplankton projections from NEMO-ERSEM and the CMIP6 models used here broadly agree, resulting in similar projections to future supportable fish biomass in the NE Atlantic (Figure 4). However, NEMO-ERSEM projections include areas of finer-scale increases to supportable fish biomass which are not captured by CMIP6 (Figure 4b and c). Notwithstanding these issues, there is broad agreement amongst models that the zooplankton trophic level supporting fish (i.e. directly as prey or indirectly as prey of prey), has declined already over most of the fishing grounds in this area (Figure 4d). Likewise, there is broad model consensus over the overall magnitude of change (Figure 4e).

3 Discussion

Our global maps (Figure 2) estimate declines in the biomass of fish that can be supported from projected reductions of phytoplankton. Global inequalities in the socioeconomic importance of capture fisheries [30, 40] leave nations who rely more on fisheries disproportionately vulnerable to socioeconomic losses and damages from fisheries declines. Our vulnerability maps therefore highlight global hotspots of fishing grounds which are heavily relied upon for socioeconomic security (Figure 3c). Our risk mapping approach (Figure 3d) identifies marine regions with high declines in projected fish biomass which coincide with high present-day pelagic fishing effort, that are important for the socioeconomic security of the nations fishing there. Spatial unevenness in the global distribution of projected fish biomass declines combined with present-day fishing patterns and inequalities in the socioeconomic importance of fishing grounds reveal a highly uneven spatial distribution of fisheries climate risks (Figure 3d). Uneven spatial distributions of risks highlight the disproportionate potential for losses and damages in nations who fish in high-risk regions.

To maintain trust in climate projections for global- and regional-level policymaking, it is important to highlight caveats [41]. A key uncertainty of our approach is whether the relationship between chlorophyll-a and the size spectra slopes, which underpin our projections [8], will hold under future environmental conditions. Atkinson et al. [8] used a diverse variety of natural aquatic ecosystems across the globe to determine the relationship between size spectra slopes and chlorophyll-a, and it is important to note that these ecosystems were already facing climate change effects, increasing confidence that the relationship will not change with continued warming. Furthermore, our Northeast Atlantic case study provides further reassurance that, at least for this region, our projections are in line with both historical observations of declining zooplankton biomass and regional-scale climate model outputs (Figure 4).

The common approach to projecting change in fish biomass under climate change is via ensembles of various ecosystem models which are fed from the outputs of Earth System models [6]. The component ecosystem models take varying approaches

to modelling the impacts of warming on complex, multiple predator-prey interactions and consumer physiology. Unlike our empirical size-based approach, these more mechanistic models have the advantage of modelling turnover rates, but on the downside the poor understanding of food web interactions leads to very poor consensus across ensembles of models [17, 18]. Our size spectrum approach offers a complementary alternative to ecosystem models which does not require poorly constrained information on temperature sensitivities of multiple processes and how these may or not adapt on climate change timescales. These size-based empirical projections instead have an intuitive simplicity that reduced phytoplankton biomass translates to reduced fish biomass (see SI Figure 1 for projected confidence intervals). However, our approach is necessarily macroscale, and does not address threats to individual fish species with specific responses to warming [42]. While our underlying relationship between size spectrum slope and Chlorophyll-a concentration is based on in-situ ecosystems already coping with multiple stressors of climate change, we do not address localised or acute factors, such as marine heatwaves [43, 44], de-oxygenation [3], or overfishing [45, 46], all of which reduce fish biomass and may interact.

Global landings from capture fisheries average around 90 million tonnes per year [1], providing a key source of high-quality lipids and proteins for human consumption [47, 48], generating income for coastal communities, as well as providing employment to over 30 million people [1, 49]. Projected declines in fish biomass (Figure 2) can therefore impact directly on high-quality food supply and economic security in many regions (Figure 3). We assessed fisheries socioeconomic losses and damages in terms of food security, employment opportunities and national GDP contributions from fish landings, but additional ecosystem services provided by fisheries are likely to be impacted, such as cultural linkages with fishing industries [50, 51]. These cultural services can be challenging to tangibly link to ecosystem change [52], but remain important in decision-making [53]. Additionally, while our projections have been interpreted in the context of capture fisheries, marine fishes provide a range of other valuable ecosystem services [50, 51, 54]. A key ecosystem service provided by fish is a global contribution to climate regulation through carbon sequestration; fish contribute around 12% of total marine carbon export and a relatively high proportion of this exported carbon is sequestered [55]. Our projections of declining fish biomass (Figure 2) therefore indicate the potential for a broad range of future marine ecosystem service declines and subsequent societal losses and damages.

The true extent of future climate losses and damages, including from projected fish biomass declines, will depend primarily on international progress in reducing net greenhouse gas emissions (Figures 1 and 2). Our fish biomass projections (Figure 2) estimate an opportunity to avoid around 10% of projected global fish biomass declines by the end of this century, through strong emission mitigation (SSP 1-2.6) compared to a high emissions pathway (SSP 5-8.5). Projections of global fish biomass declines (Figure 2; [6, 15]) therefore add to a growing body of evidence on hazardous climate effects [56], providing further motivation for international decision-makers to meet emissions targets. Alongside international discussions on mitigating greenhouse gas

emissions, decision-makers can also mitigate fisheries climate risks through reducing compounding pressures on fish stocks [57].

While progress towards global emissions targets is constrained by ongoing international negotiations and policy developments, other human pressures on fisheries, such as nutrient pollution, habitat destruction, and overfishing, are relatively more manageable. Our risk mapping approach (Figure 3d) therefore provides a unique perspective of priority marine regions for reducing human pressures on fisheries, where efforts to mitigate fish stock declines could avoid socioeconomic losses and damages. A key mitigation measure could include shifts to more sustainable fishing practices, such as balanced harvesting [58], and ensuring that over-fishing is avoided, given projected declines in supportable fish biomass (Figure 2) are expected to reduce the baselines levels of sustainable exploitation. With these risks also being intense in some Areas Beyond National Jurisdiction (the High Seas) (Figure 3d), the developing High Seas Treaty [59] provides a valuable opportunity to develop international agreements which ensure fish stocks are not over-exploited in both high climate risk (Figure 3d) and socioeconomically important (Figure 3c) High Seas fishing grounds. In addition, the High Seas treaty could prioritise the development of marine protected areas [60] designed to benefit fisheries in regions we have identified as high-risk. Some of the highest-risk fishing grounds identified in this paper, including Southeast Asia and the western coasts of Africa and South America are known hotspots for untracked fishing vessels [61], highlighting the challenges of managing illegal and unregulated fishing activities [61, 62] in some of these regions.

Alongside reducing the severity of fish biomass declines through greenhouse gas mitigation and effective ecosystem management, fisheries climate risks can be reduced with adaptation measures aimed at reducing the vulnerability of communities to fish biomass declines (Figure 1). Addressing global inequalities in the socioeconomic dependence of individual countries on fisheries, however, is beyond the scope of our work. Previous studies have begun to address country-level fisheries projections and climate vulnerability analyses [30, 32, 63–65], providing valuable evidence to support decision-makers to reduce national vulnerability to fisheries declines, such as the Sustainable Development Goal for prioritising sustainable fisheries management in Small Island Developing States (target 14.7; [66]).

We also reveal priority areas where reducing the exposure (Figures 1 and 3b) of fisheries to fish biomass declines could further reduce socioeconomic risks (Figure 3d). This could take the form of both overall reductions in fishing effort (which will depend on progress in reducing socioeconomic dependence on fisheries) and spatially managing fisheries based on the projected change in the supportable fish biomass (Figures 2 and 3a), to align fisheries yields with the ecosystem's capacity to sustainably produce food [67]. As continued ocean warming drives the redistribution of marine species, fishing effort is predicted to move poleward to track changes in the distribution of commercially valuable fish species [34]. An unmanaged redistribution of fishing effort could increase the intensity of fishing in sensitive habitats, exacerbating marine biodiversity

loss [68] and threatening future ecosystem service provision [69]. Further consideration is therefore needed to understand which low risk regions (Figure 3d) could be suitable for increased future fishing effort and how wider management measures should be targeted to ensure sustainable stock management in these regions [58, 60]. The spatial resolution of our global-scale risk assessments (based on CMIP6 models) does not capture fine-scale fisheries risks (Figure 3), future work could therefore make use of regional-scale models, such as NEMO-ERSEM (Figure 4), coupled with fine-scale fisheries data [70], to assess fisheries climate risks at the required spatial resolution to guide local scale fisheries management and support exposure reduction in small scale fisheries.

4 Methods

4.1 Principle of using size spectrum slopes to estimate the supportable biomass of fish

Body size is an important trait in pelagic ecosystems, exerting control on key biological functions such as prey size and physiological rates [24, 71]. The slopes of Normalised Body Mass Size Spectra ([72]; hereafter "size spectrum slopes") provide an index of the relative abundance of small and large pelagic organisms and therefore help to quantify the efficiency of mass transfer to large consumers [19]. Sprules and Munawar [73], Rossberg et al. [21] and Atkinson et al. [8] all found that systematic changes in size spectrum slopes across aquatic ecosystems related to their nutrient status. Atkinson et al. [8] further found that these size spectrum slopes did not relate to temperature as some have suggested, but only to the nutrient status of the systems, such that systems with low average Chl-*a* had steeply negative slopes (i.e. inefficient food webs) while those with higher Chl-*a* had less steep slopes and thus more efficient food webs. Importantly, these findings are all at the macroscale (i.e. of globally-distributed in-situ ecosystems), with each presumably adapting to multiple stressors. For this reason, Atkinson et al. [8] used the relationship between size spectrum slope and annual mean Chl-*a* concentration in a space-for time substitution approach, to estimate changes in size spectrum slope based on modelled changes in Chl-*a* derived by Earth System models. Since size spectrum slopes are broadly linear across the broad size spectrum of pelagic life [74], the size spectrum slope can be further used to estimate the supportable biomass of fish based on changes in modelled phytoplankton biomass [8].

Chl-*a* concentration (mg Chl-*a* m^{-3}) and depth-integrated phytoplankton biomass (g C m^{-2}) were obtained from GFDL-ESM4 and IPSL-CM6A-LR, two Earth System Models from the Coupled Model Intercomparison Project Phase 6 (CMIP6; [75]). These Earth System Models were selected because they are characterised by a very different Equilibrium Climate Sensitivity (ECS), with IPSL-CM6A-LR being one of the most sensitive (ECS=4.6°C) and GFDL-ESM4 one of the least sensitive (ECS=2.6°C) [76]. Both models provided monthly, global-scale data at 1° spatial resolution for the historical period 1970-2014, and for 2015-2099 under both low (SSP 1-2.6) and high emission scenarios (SSP5-8.5). Chlorophyll-a and phytoplankton

biomass values were averaged across the two Earth System Models, then averaged temporally for the periods 1990-1999 and decadal intervals between 2040 and 2099.

To provide an independent approach for a well-studied area, the NE Atlantic/NW European shelf, outputs from a higher resolution model were also used. A downscaled projection driven by the Earth System Model IPSL-CM5-MR under the RCP8.5 scenario using the NEMO-ERSEM coupled model system on the Atlantic Margin Model at 7Km resolution (AMM7) was used [77]. NEMO [78] is a hydrodynamic model and ERSEM is an intermediate complexity ecosystem model with 3 zooplankton and 4 phytoplankton groups [39]. Outputs from the original 7km grid were aggregated on the common 1-degree grid before analysing them. The AMM7 NEMO-ERSEM modelling system has been used to assess impact of climate change on the Northeast Atlantic in several studies [77, 79, 80], including in the Ocean Acidification assessment included in the last Quality Status Report of OSPAR [81].

Mean decadal Normalised Biomass Size Spectra slopes (S) were then calculated from projected mean decadal Chlorophyll-*a* (Chl-*a*) values using the relationship derived in the meta-analysis of Atkinson et al. [8] (equation 1). This empirical relationship was calculated from size spectrum slopes compiled from 41 distinct ecosystems ranging 600-fold in mean Chl-*a* values.

$$S = -0.0065\,(log10\,[Chla])^2 + 0.0663\,(log10\,[Chla]) - 1.10651 \tag{1}$$

Following the approach of Atkinson et al. [8], our projected decadal averages of Normalised Biomass Size Spectra slopes (S values, equation 1) and projected phytoplankton biomass values (mg C m^{-2}) were used to project the total supportable fish biomass. This approach represents plankton as the size range 0.5 to 50,000 pg C and fish 0.5 g C to 50,000 g C [74]. To estimate the relative changes in biomass of fish size range compared to the phytoplankton size range, projected size spectra slope (S) is used to extrapolate projected phytoplankton biomass. Equation 2 summarises this approach, where the size range of fish is represented as 12 orders of magnitude greater than the phytoplankton size range. Percentage change to supportable fish biomass from 1990 – 1999 were calculated as the difference between the means of decadal intervals between 2040 and 2100.

$$\textit{Supportable fish biomass} = (4.99995 \times 10^4) \times 10^{(12[S]+\log_{10}\left[\frac{\text{Phytoplankton biomass}}{4.99995\times10^{-1}}\right])} \tag{2}$$

4.2 Risk assessment of fishing grounds

4.2.1 Hazard metric: rate of declines of fish biomass

Decadal projected percentage changes in supportable fish biomass (relative to 1990-1999, see method above) were converted to rates of change in supportable fish biomass, using a least-squares linear regression (forced through the origin) for each grid-cell.

Rates of change were filtered to only include regions of projected declining fish biomass, converted to positive values (multiplied by -1), and normalised between 0 and 1 using equation 3. Our metric normalisation approach meant that we assessed relative, rather than absolute, hazard (and risk). We therefore did not compare risks under different emissions pathways, but only included SSP 5-8.5 due to similar spatial distributions of relative fish biomass declines under each emission scenario (see SI Figure 6 for risk comparison between SSP 1-2.6 and 5-8.5). For visualisation purposes, the fisheries hazard metric was transformed using $y = x^{0.15}$ to produce Figure 3a, before renormalising between 0 and 1.

$$y = \frac{x - \text{minimum}(x)}{\text{maximum}(x) - \text{minimum}(x)} \tag{3}$$

4.2.2 Exposure metric: present day fishing effort

Patterns of present day pelagic fishing effort were sourced from the database provided in Rousseau et al. [82]. While other fishing effort datasets are freely available, such as from automatic identification systems (AIS) [70], the database from Rousseau et al. [82] provides data in regions with poor AIS data coverage, such as Southeast Asia [61], making it more appropriate for our global approach. Total annual average country-aggregated nominal fishing effort (Kw-h km^{-2} y^{-1}) was processed for the most recent three years available (2014 – 2017). Fishing effort was filtered to activities targeting pelagic fish taxa (full size range) given the size spectra relationship derived in Atkinson et al. [8] (which underpins our fish biomass projections) are less likely to be directly linked to other fish functional groups, such as benthic taxa, and would risk introducing extra uncertainty into our analyses. Our exposure and risk maps therefore underestimate risks in fishing regions intensive fisheries targeting other fish groups, such as demersal fisheries. While Rousseau et al. [82] provide data for the effective fishing effort (nominal effort corrected for relative developments in catch efficiency between countries), we opted to use nominal fishing effort due to its comparability to other available fishing databases, including AIS databases. The country-aggregated mean total annual fishing effort was then normalised to a score between 0 and 1 for each grid cell using equation 3.

4.2.3 Vulnerability metric: socioeconomic dependence on fishing grounds

A vulnerability metric for each country was calculated according to the fisheries dependency metric presented in Blanchard et al. [63] and Barange et al. [32]. The metric represents the socioeconomic dependence of each country on fisheries, calculated from a mean of three equally weighted indices standardised between 0 and 1: the economic contributions of fish landings, the employment contributions of fisheries, and the food security provided by fisheries.

Percentage total GDP contributions from fish landings were calculated using the mean total annual fish landings between 2015-2019 from the SeaAroundUs database [83] and the 2015-2019 average GDP values from the World Bank [84]. Eritrea and

Venezuela did not have GDP data available for 2015-2019, so we used the most recently available GDP values (for the year 2011 for Eritrea and 2014 for Venezuela). Percentage workforce employment in the fisheries sector by country was calculated from the employment in fishing and agriculture indicator from the Food and Agriculture Organisation's FAOSTAT database [85] and total working population (ages 15-64) values from the International Labour Organization's ILOSTAT database [86], using the most recent year of data available for each value and country. Fisheries contributions to food security were calculated from equation 4, as presented in Blanchard et al. [63] and Barange et al. [32], using updated country dietary profile data provided in Nash et al. [65]. A standard required animal protein intake value of 36 grams per capita per day was used [87], keeping our approach in-line with previous studies [32, 63].

$$\text{Food security index} = \frac{\left(\frac{\text{Fish protein intake}}{\text{Total animal protein intake}}\right)}{\left(\frac{\text{Total animal protein intake}}{\text{Required animal protein intake}}\right)} \tag{4}$$

Due to data availability issues, we calculated vulnerability metrics for countries which did not have all three indices available (by taking a mean average of the available indices), before renormalising between 0 and 1. 207 countries had data available for at least one of the indices, whereas 110 countries had data available for all three indices. This approach is likely to skew the vulnerability indicators calculated for countries with indices missing (the three vulnerability indices are not necessarily strongly auto-correlated) but provides a precautionary assessment solution [53], given the data available. Data could not be sourced for dietary, economic and employment indices specific to pelagic marine fisheries so we used data for all fisheries (e.g., demersal and in some cases freshwater). Our vulnerability metric may therefore overestimate the socioeconomic dependency on pelagic fisheries in some countries but is minimised in the final vulnerability metric (see below) by weighting each grid-cell's mean vulnerability by each country's pelagic fishing intensity.

To link the socioeconomic vulnerability data to patterns of fishing effort and assess the socioeconomic vulnerability of fishing grounds to climate effects, a metric was designed to represent the contributions of global fishing grounds to the socioeconomic security of the countries who fish within them. Country-level values of mean total annual (2014-2017) pelagic fishing intensity (days) per grid-cell were sourced from Rousseau et al. [82]. For each grid-cell, country-level pelagic fishing intensities were multiplied by the country's corresponding vulnerability metric and divided by the total fishing intensity (equation 5), essentially capturing the average socioeconomic vulnerability metric weighted by the country's fishing intensity in the region.

$$\text{Vulnerability} = \frac{\sum(\text{Total pelagic fishing days by country} \times \text{Country vulnerability metric})}{\sum(\text{Total pelagic fishing days by country})} \tag{5}$$

Limitations in data availability resulted in some missing vulnerability metrics for countries with available fishing data in Rousseau et al. [82]. To represent regions with poor data coverage, grid-cells with over 50% of fishing intensity with missing country-level vulnerability metrics were removed and marked as missing data in our figures. In addition, the EEZs of countries with missing fishing data in Rousseau et al. [82] were also marked as missing data.

4.2.4 Risk mapping

A fisheries climate risk indicator for each grid-cell was calculated by equation 6 with our three fisheries climate risk assessment metrics: rate of decline of fish biomass (hazard), present day fishing effort (exposure), and socioeconomic dependence on fishing grounds (vulnerability). Equation 6 is based on definitions of risk from the International Panel on Climate Change [88]. Metrics were all equally weighted and the final risk indicator value was transformed using $y = x^{0.15}$ for visualisation purposes, before renormalising between 0 and 1 using equation 3.

$$\text{Risk} = \text{Hazard} \times \text{Exposure} \times \text{Vulnerability} \tag{6}$$

4.3 Historical zooplankton biomass trends

To provide a context and sense-check for the projections of changes in supportable biomass of fish we examine past changes in a well sampled region, the NE Atlantic, over the last 65 years which included phases of rapid warming [36, 89]. There were no total fish biomass data available over sufficiently large temporal and spatial scales, and the nearest trophic levels to fish with a suitable high-quality dataset were zooplankton from the Continuous Plankton Recorder (CPR) Survey (www.cprsurvey.org). Here, and for the first time, we have estimated long-term trends in total zooplankton biomass over the large areas covered by this sampling instrument.

To do this, zooplankton abundance counts per sample (i.e. no. $3m^3$) between 1958 – 2021 were provided by the Continuous Plankton Recorder survey (www.cprsurvey.org, dataset: https://doi.org/10.17031/67ebed65bd6f9). The abundance data were multiplied by their respective carbon mass estimations provided in a new database [90] and then summed to obtain total biomass (µg per $3m^3$). The data were log transformed using Log_{10} (µg per $3m^3$+1) in order to homogenise the variance and reduce the influence of zero counts [91]. These biomass data were then gridded onto a 1° x 1° grid, using the monthly mean value for each grid cell, and only using grid cells with $\geq$ 3 samples to reduce the potential impact of low sampling effort [91]. To visualise the changes within the Northeast Atlantic, the data were interpolated using an objective mapping technique, described by equation 7:

$$b = w \times E^{-1} \times r \tag{7}$$

where, b is the mapped property, w is the data weights, E is the covariance matrix and r is the residuals (weighted mean) [92].

Supplementary information. Supplementary figures and country-level fisheries dependency metrics can be found in the supplementary file accompanying this manuscript.

Acknowledgements. MPF acknowledges funding from the UK Department for Environment, Food and Rural Affairs (DEFRA), the University of Plymouth, and The Alan Turing Institute Enrichment Scheme. AMG, CO and MH acknowledge funding through the marine arm of the DEFRA Natural Capital and Ecosystem Assessment (NCEA) programme (NC34 Pelagic program - "PelCap"). AA was also funded through the European Space Agency ESA Cluster Multistressors Impact on Ocean Health grant number 4000142100/I-DT project Multiple Threats on Ocean Health (MiTHO) and through the NERC AtlantiS programme. JAFS contribution has been funded through the H2020 project OBAMA-NEXT (#101081642), as well as BioBoost+ project within the Biodiversa+ European Biodiversity Partnership program. Funded by the Europea Union. YA acknowledges funding from European Union's Horizon 2020 research and innovation programme under grant agreement no. 820989 (project COMFORT), and from the NERC projects RECICLE (NE/M004120/1) and FOCUS (NE/X006271/1). MSAT was supported via the Natural Environment Research Council and the Economic and Social Research Council grant NE/V017039/1. Views and opinions expressed are however those of the author(s) only and do not necessarily reflect those of the funders.

Data availability statement. All code used to generate the figures in this paper can be found at: https://github.com/matthewpfaith/FishRisk. Earth system model outputs can be found at: https://data.isimip.org/. For all other data, including socioeconomic and fishing effort data, please see the methods section.

Conflict of interest. None declared.

Author contributions. Conceived and designed the study: MPF and AA. Analyzed the data: MPF, CO, and AA. Wrote the paper: MPF, AA, RH, CO, JAFS, CSP, YA, KS, SR, MT, MH, and AMG.

References

[1] FAO. The state of world fisheries and aquaculture 2024 – blue transformation in action. (2024). URL https://doi.org/10.4060/cd0683en.

[2] Halpern, B. S. *et al.* A global map of human impact on marine ecosystems. *Science* **319**, 948–952 (2008).

[3] Limburg, K. E., Breitburg, D., Swaney, D. P. & Jacinto, G. Ocean deoxygenation: a primer. *One Earth* **2**, 24–29 (2020). URL https://doi.org/10.1016/j.oneear.2020.01.001.

[4] Du Pontavice, H., Gascuel, D., Reygondeau, G., Maureaud, A. & Cheung, W. W. Climate change undermines the global functioning of marine food webs. *Global Change Biology* **26**, 1306–1318 (2020). URL https://doi.org/10.1111/gcb.14944.

[5] Tagliabue, A. *et al.* Persistent uncertainties in ocean net primary production climate change projections at regional scales raise challenges for assessing impacts on ecosystem services. *Frontiers in Climate* **3**, 738224 (2021). URL https://doi.org/10.3389/fclim.2021.738224.

[6] Tittensor, D. P. *et al.* Next-generation ensemble projections reveal higher climate risks for marine ecosystems. *Nature Climate Change* **11**, 973–981 (2021). URL https://doi.org/10.1038/s41558-021-01173-9.

[7] Cinner, J. E. *et al.* Potential impacts of climate change on agriculture and fisheries production in 72 tropical coastal communities. *Nature communications* **13**, 3530 (2022). URL https://doi.org/10.1038/s41467-022-30991-4.

[8] Atkinson, A. *et al.* Steeper size spectra with decreasing phytoplankton biomass indicate strong trophic amplification and future fish declines. *Nature Communications* **15**, 381 (2024). URL https://doi.org/10.1038/s41467-023-44406-5.

[9] Irwin, A. J. & Oliver, M. J. Are ocean deserts getting larger? *Geophysical Research Letters* **36** (2009). URL https://doi.org/10.1029/2009gl039883.

[10] Leonelli, F. *et al.* Ultra-oligotrophic waters expansion in the north atlantic subtropical gyre revealed by 21 years of satellite observations. *Geophysical Research Letters* **49**, e2021GL096965 (2022). URL https://doi.org/10.1029/2021gl096965.

[11] Li, G. *et al.* Increasing ocean stratification over the past half-century. *Nature Climate Change* **10**, 1116–1123 (2020). URL https://doi.org/10.1038/s41558-020-00918-2.

[12] Kwiatkowski, L. *et al.* Twenty-first century ocean warming, acidification, deoxygenation, and upper-ocean nutrient and primary production decline from cmip6 model projections. *Biogeosciences* **17**, 3439–3470 (2020). URL https://doi.org/10.5194/bg-17-3439-2020.

[13] Schmidt, K. *et al.* Increasing picocyanobacteria success in shelf waters contributes to long-term food web degradation. *Global Change Biology* **26**, 5574–5587 (2020). URL https://doi.org/10.1111/gcb.15161.

[14] Tittensor, D. P. *et al.* A protocol for the intercomparison of marine fishery and ecosystem models: Fish-mip v1.0. *Geoscientific Model Development* **11**, 1421–1442 (2018). URL https://doi.org/10.5194/gmd-11-1421-2018.

[15] Blanchard, J. L. & Novaglio, C. Climate change risks to marine ecosystems and fisheries – projections to 2100 from the fisheries and marine ecosystem model

intercomparison project. (2024). URL https://doi.org/10.4060/cd1379en.

[16] Blanchard, J. L. *et al.* Detecting, attributing, and projecting global marine ecosystem and fisheries change: Fishmip 2.0. *Earth's Future* **12**, e2023EF004402 (2024). URL https://doi.org/10.1029/2023ef004402.

[17] Eddy, T. D. *et al.* Global and regional marine ecosystem models reveal key uncertainties in climate change projections. *Earth's Future* **13**, e2024EF005537 (2025).

[18] Heneghan, R. F. *et al.* Disentangling diverse responses to climate change among global marine ecosystem models. *Progress in Oceanography* **198**, 102659 (2021). URL https://doi.org/10.1016/j.pocean.2021.102659.

[19] Sprules, W. G. & Barth, L. E. Surfing the biomass size spectrum: some remarks on history, theory, and application. *Canadian Journal of Fisheries and Aquatic Sciences* **73**, 477–495 (2016). URL https://doi.org/10.1139/cjfas-2015-0115.

[20] Armengol, L., Calbet, A., Franchy, G., Rodríguez-Santos, A. & Hernández-León, S. Planktonic food web structure and trophic transfer efficiency along a productivity gradient in the tropical and subtropical atlantic ocean. *Scientific reports* **9**, 2044 (2019). URL https://doi.org/10.1038/s41598-019-38507-9.

[21] Rossberg, A. G., Gaedke, U. & Kratina, P. Dome patterns in pelagic size spectra reveal strong trophic cascades. *Nature communications* **10**, 4396 (2019). URL https://doi.org/10.1038/s41467-019-12289-0.

[22] Heneghan, R. F., Hatton, I. A. & Galbraith, E. D. Climate change impacts on marine ecosystems through the lens of the size spectrum. *Emerging Topics in Life Sciences* **3**, 233–243 (2019). URL https://doi.org/10.1042/etls20190042.

[23] Russo, L. *et al.* Long-term oscillations in the normalized biomass-size spectrum reveal the impact of oligotrophication on zooplankton trophic structure in the north atlantic subtropical gyre. *Marine Environmental Research* **193**, 106295 (2024). URL https://doi.org/10.1016/j.marenvres.2023.106295.

[24] Blanchard, J. L., Heneghan, R. F., Everett, J. D., Trebilco, R. & Richardson, A. J. From bacteria to whales: using functional size spectra to model marine ecosystems. *Trends in ecology & evolution* **32**, 174–186 (2017). URL https://doi.org/10.1016/j.tree.2016.12.003.

[25] IPCC. *Climate Change 2022 – Impacts, Adaptation and Vulnerability: Working Group II Contribution to the Sixth Assessment Report of the Intergovernmental Panel on Climate Change* (Cambridge University Press, Cambridge, 2023). URL https://www.cambridge.org/core/product/161F238F406D530891AAAE1FC76651BD. (IPCC).

[26] on Climate Change (IPCC), I. P. *Point of Departure and Key Concepts*, 121–196 (Cambridge University Press, 2023). URL https://doi.org/10.1017/9781009325844.003.

[27] Vousdoukas, M. I. *et al.* Small island developing states under threat by rising seas even in a 1.5 c warming world. *Nature sustainability* **6**, 1552–1564 (2023). URL https://doi.org/10.1038/s41893-023-01230-5.

[28] van der Geest, K. *et al.* The impacts of climate change on ecosystem services and resulting losses and damages to people and society. *Loss and damage from climate change: Concepts, methods and policy options* 221–236 (2019). URL https://doi.org/10.1007/978-3-319-72026-5_9.

[29] Janzen, S., Emerton, L., van der Geest, K., Narvaez, L. & Sebesvari, Z. Assessing losses and damages to ecosystem services: current state and opportunities for the warsaw international mechanism under the unfccc. *Climate Policy* **21**, 912–926 (2021). URL https://doi.org/10.1080/14693062.2021.1947177.

[30] Boyce, D. G., Lotze, H. K., Tittensor, D. P., Carozza, D. A. & Worm, B. Future ocean biomass losses may widen socioeconomic equity gaps. *Nature Communications* **11**, 2235 (2020). URL https://doi.org/10.1038/s41467-020-15708-9.

[31] Oremus, K. L. *et al.* Governance challenges for tropical nations losing fish species due to climate change. *Nature Sustainability* **3**, 277–280 (2020). URL https://doi.org/10.1038/s41893-020-0476-y.

[32] Barange, M. *et al.* Impacts of climate change on marine ecosystem production in societies dependent on fisheries. *Nature climate change* **4**, 211–216 (2014). URL https://doi.org/10.1038/nclimate2119.

[33] Tickler, D., Meeuwig, J. J., Palomares, M.-L., Pauly, D. & Zeller, D. Far from home: Distance patterns of global fishing fleets. *Science advances* **4**, eaar3279 (2018). URL https://doi.org/10.1126/sciadv.aar3279.

[34] Cruz, L., Pennino, M. & Lopes, P. Fisheries track the future redistribution of marine species. *Nature Climate Change* 1–8 (2024). URL https://doi.org/10.1038/s41558-024-02127-7.

[35] Reid, P. C., Colebrook, J., Matthews, J., Aiken, J. & Team, C. P. R. The continuous plankton recorder: concepts and history, from plankton indicator to undulating recorders. *Progress in Oceanography* **58**, 117–173 (2003). URL https://doi.org/10.1016/j.pocean.2003.08.002.

[36] Chust, G. *et al.* Cross-basin and cross-taxa patterns of marine community tropicalization and deborealization in warming european seas. *Nature communications* **15**, 2126 (2024). URL https://doi.org/10.1038/s41467-024-46526-y.

[37] Watson, R. A. *et al.* Global marine yield halved as fishing intensity redoubles. *Fish and Fisheries* **14**, 493–503 (2013). URL https://doi.org/10.1111/j.1467-2979.2012.00483.x.

[38] Queirós, A. M., Fernandes, J., Genevier, L. & Lynam, C. P. Climate change alters fish community size-structure, requiring adaptive policy targets. *Fish and Fisheries* **19**, 613–621 (2018). URL https://doi.org/10.1111/faf.12278.

[39] Butenschön, M. *et al.* Ersem 15.06: a generic model for marine biogeochemistry and the ecosystem dynamics of the lower trophic levels. *Geoscientific Model Development* **9**, 1293–1339 (2016). URL https://doi.org/10.5194/gmd-9-1293-2016.

[40] Belhabib, D., Sumaila, U. R. & Pauly, D. Feeding the poor: Contribution of west african fisheries to employment and food security. *Ocean Coastal Management* **111**, 72–81 (2015). URL https://doi.org/10.1016/j.ocecoaman.2015.04.010.

[41] Dries, C., McDowell, M., Rebitschek, F. G. & Leuker, C. When evidence changes: Communicating uncertainty protects against a loss of trust. *Public Understanding of Science* **33**, 777–794 (2024). URL https://doi.org/10.1177/09636625241228449.

[42] Thompson, M. S., Couce, E., Schratzberger, M. & Lynam, C. P. Climate change affects the distribution of diversity across marine food webs. *Global Change Biology* **29**, 6606–6619 (2023). URL https://doi.org/10.1111/gcb.16881.

[43] Cheung, W. W. *et al.* Marine high temperature extremes amplify the impacts of climate change on fish and fisheries. *Science Advances* **7**, eabh0895 (2021). URL https://doi.org/10.1126/sciadv.abh0895.

[44] Hobday, A. J. *et al.* A hierarchical approach to defining marine heatwaves. *Progress in oceanography* **141**, 227–238 (2016). URL https://doi.org/10.1016/j.pocean.2015.12.014.

[45] Link, J. S. & Watson, R. A. Global ecosystem overfishing: Clear delineation within real limits to production. *Science Advances* **5**, eaav0474 (2019). URL https://doi.org/10.1126/sciadv.aav0474.

[46] Lauria, V. *et al.* Importance of fisheries for food security across three climate change vulnerable deltas. *Science of the Total Environment* **640**, 1566–1577 (2018). URL https://doi.org/10.1016/j.scitotenv.2018.06.011.

[47] Golden, C. D. *et al.* Aquatic foods to nourish nations. *Nature* **598**, 315–320 (2021). URL https://doi.org/10.1038/s41586-021-03917-1.

[48] Boyd, C. E., McNevin, A. A. & Davis, R. P. The contribution of fisheries and aquaculture to the global protein supply. *Food security* **14**, 805–827 (2022). URL

https://doi.org/10.1007/s12571-021-01246-9.

[49] Garcia, S. M. & Rosenberg, A. A. Food security and marine capture fisheries: characteristics, trends, drivers and future perspectives. *Philosophical Transactions of the Royal Society B: Biological Sciences* **365**, 2869–2880 (2010). URL https://doi.org/10.1098/rstb.2010.0171.

[50] Urquhart, J. & Acott, T. A sense of place in cultural ecosystem services: The case of cornish fishing communities. *Society Natural Resources* **27**, 3–19 (2014). URL https://doi.org/10.1080/08941920.2013.820811.

[51] López de la Lama, R., de la Puente, S., Sueiro, J. C. & Chan, K. M. Reconnecting with the past and anticipating the future: A review of fisheries-derived cultural ecosystem services in pre-hispanic peru. *People and Nature* **3**, 129–147 (2021). URL https://doi.org/10.1002/pan3.10153.

[52] Jones, L. *et al.* Can we model cultural ecosystem services, and are we measuring the right things? *People and Nature* **4**, 166–179 (2022). URL https://doi.org/10.1002/pan3.10271.

[53] Niner, H. J., Morgera, E., Longo, A., Howell, K. L. & Rees, S. E. Connecting ecosystem services research and human rights to revamp the application of the precautionary principle. *npj Ocean Sustainability* **3**, 35 (2024). URL https://doi.org/10.1038/s44183-024-00072-8.

[54] Nissar, S. *et al.* A review of the ecosystem services provided by the marine forage fish. *Hydrobiologia* (2023). URL https://doi.org/10.1007/s10750-022-05033-1.

[55] Pinti, J. *et al.* Model estimates of metazoans' contributions to the biological carbon pump. *Biogeosciences* **20**, 997–1009 (2023). URL https://doi.org/10.5194/bg-20-997-2023.

[56] Mora, C. *et al.* Broad threat to humanity from cumulative climate hazards intensified by greenhouse gas emissions. *Nature climate change* **8**, 1062–1071 (2018). URL https://doi.org/10.1038/s41558-018-0315-6.

[57] Lam, V. W. *et al.* Climate change, tropical fisheries and prospects for sustainable development. *Nature Reviews Earth Environment* **1**, 440–454 (2020). URL https://doi.org/10.1038/s43017-020-0071-9.

[58] Law, R. & Plank, M. J. Fishing for biodiversity by balanced harvesting. *Fish and fisheries* **24**, 21–39 (2023). URL https://doi.org/10.1111/faf.12705.

[59] BBNJ. Agreement on biodiversity beyond national jurisdiction (2023). URL https://www.un.org/bbnj.

[60] Anabitarte, A. *et al.* The use of atlantic seascapes for marine protected areas planning in the context of the marine biological diversity of areas beyond national jurisdiction agreement. *Marine Pollution Bulletin* **214**, 117776 (2025). URL https://doi.org/10.1016/j.marpolbul.2025.117776.

[61] Paolo, F. S. *et al.* Satellite mapping reveals extensive industrial activity at sea. *Nature* **625**, 85–91 (2024). URL https://doi.org/10.1038/s41586-023-06825-8.

[62] Park, J. *et al.* Illuminating dark fishing fleets in north korea. *Science advances* **6**, eabb1197 (2020). URL https://doi.org/10.1126/sciadv.abb1197.

[63] Blanchard, J. L. *et al.* Linked sustainability challenges and trade-offs among fisheries, aquaculture and agriculture. *Nature ecology evolution* **1**, 1240–1249 (2017). URL https://doi.org/10.1038/s41559-017-0258-8.

[64] Payne, M. R., Kudahl, M., Engelhard, G. H., Peck, M. A. & Pinnegar, J. K. Climate risk to european fisheries and coastal communities. *Proceedings of the National Academy of Sciences* **118**, e2018086118 (2021). URL https://doi.org/10.1073/pnas.2018086118.

[65] Nash, K. L. *et al.* Trade and foreign fishing mediate global marine nutrient supply. *Proceedings of the National Academy of Sciences* **119**, e2120817119 (2022). URL https://doi.org/10.1073/pnas.2120817119.

[66] UN. United nations sustainable development goals (2015). URL https://sdgs.un.org/goals/goal14#overview.

[67] Robinson, J. P. *et al.* Managing fisheries for maximum nutrient yield. *Fish and Fisheries* **23**, 800–811 (2022). URL https://doi.org/10.1111/faf.12649.

[68] Dureuil, M., Boerder, K., Burnett, K. A., Froese, R. & Worm, B. Elevated trawling inside protected areas undermines conservation outcomes in a global fishing hot spot. *Science* **362**, 1403–1407 (2018). URL https://doi.org/10.1126/science.aau0561.

[69] Worm, B. *et al.* Impacts of biodiversity loss on ocean ecosystem services. *science* **314**, 787–790 (2006).

[70] Kroodsma, D. A. *et al.* Tracking the global footprint of fisheries. *Science* **359**, 904–908 (2018). URL https://doi.org/10.1126/science.aao5646.

[71] Platt, T. The structure of pelagic marine ecosystems. *Rpp. P.-v. Cons. int. Explor. Mer.* **173**, 60–65 (1978).

[72] Platt, T. & Denman, K. Organisation in the pelagic ecosystem. *Helgoländer Wissenschaftliche Meeresuntersuchungen* **30**, 575–581 (1977). URL https://doi.org/10.1007/bf02207862.

[73] Sprules, W. G. & Munawar, M. Plankton size spectra in relation to ecosystem productivity, size, and perturbation. *Canadian Journal of Fisheries and Aquatic Sciences* **43**, 1789–1794 (1986). URL https://doi.org/10.1139/f86-222.

[74] Hatton, I. A., Heneghan, R. F., Bar-On, Y. M. & Galbraith, E. D. The global ocean size spectrum from bacteria to whales. *Science Advances* **7**, eabh3732 (2021). URL https://doi.org/10.1126/sciadv.abh3732.

[75] Eyring, V. *et al.* Overview of the coupled model intercomparison project phase 6 (cmip6) experimental design and organization. *Geoscientific Model Development* **9**, 1937–1958 (2016). URL https://doi.org/10.5194/gmd-9-1937-2016.

[76] Meehl, G. A. *et al.* Context for interpreting equilibrium climate sensitivity and transient climate response from the cmip6 earth system models. *Science Advances* **6**, eaba1981 (2020). URL https://doi.org/10.1126/sciadv.aba1981.

[77] Galli, G., Wakelin, S., Harle, J., Holt, J. & Artioli, Y. Multi-model comparison of trends and controls of near-bed oxygen concentration on the northwest european continental shelf under climate change. *Biogeosciences* **21**, 2143–2158 (2024). URL https://doi.org/10.5194/bg-21-2143-2024.

[78] Madec, G. & the NEMO team. Nemo ocean engine (no. 1288-1619) (2016). URL https://www.nemo-ocean.eu/doc/.

[79] Artioli, Y. *et al.* Heterogeneity of impacts of high co 2 on the north western european shelf. *Biogeosciences* **11**, 601–612 (2014). URL https://doi.org/10.5194/bg-11-601-2014.

[80] Holt, J. *et al.* Climate-driven change in the north atlantic and arctic oceans can greatly reduce the circulation of the north sea. *Geophysical Research Letters* **45**, 11,827–11,836 (2018). URL https://doi.org/10.1029/2018gl078878.

[81] McGovern, E. *et al.* Ocean acidification thematic assessment, in: Ospar commission (ed.). *The 2023 Quality Status Report for the North-east Atlantic.* (2022). URL https://oap.ospar.org/en/ospar-assessments/quality-status-reports/qsr-2023/other-assessments/ocean-acidification/.

[82] Rousseau, Y. *et al.* A database of mapped global fishing activity 1950–2017. *Scientific Data* **11**, 48 (2024). URL https://doi.org/10.1038/s41597-023-02824-6.

[83] Pauly, D., Zeller, D. & Palomares, M. E. Sea around us concepts, design and data (2020). URL seaaroundus.org.

[84] Bank, W. Gdp (current us$): Ny.gdp.mktp.cd (2025). URL https://data.worldbank.org/indicator/NY.GDP.MKTP.CD.

[85] FAO. Employment indicators: Agriculture and agrifood systems (2024). URL https://www.fao.org/faostat/en/#data/OEA.

[86] ILO. Ilostat data explorer: Employment by age and sex (thousands) - annual (2024). URL https://rshiny.ilo.org/dataexplorer20/?lang=en&id=EMP_TEMP_SEX_AGE_NB_A.

[87] Akpan, S. B., Patrick, I. V., Udoka, S. J., Offiong, E. A. & Okon, U. E. Determinants of credit access and demand among poultry farmers in akwa ibom state, nigeria (2013). URL https://doi.org/10.9734/ajea/2013/2810.

[88] Pörtner, H.-O. *et al.* The ocean and cryosphere in a changing climate. *IPCC special report on the ocean and cryosphere in a changing climate* **1155**, 10.1017 (2019). URL https://doi.org/10.1017/9781009157964.

[89] Emeis, K.-C. *et al.* The north sea—a shelf sea in the anthropocene. *Journal of Marine Systems* **141**, 18–33 (2015).

[90] Atkinson, A. *et al.* Estimates of individual carbon masses of zooplankton taxa from the ne atlantic and nw european shelf, based on ring nets and continuous plankton recorder. (2024). URL https://doi.org/10.17031/6733204cc545e.1.

[91] Helaouet, P., Beaugrand, G. & Edwards, M. Understanding long-term changes in species abundance using a niche-based approach. *PloS one* **8**, e79186 (2013). URL https://doi.org/10.1371/journal.pone.0079186.

[92] Schmidtko, S., Johnson, G. C. & Lyman, J. M. Mimoc: A global monthly isopycnal upper-ocean climatology with mixed layers. *Journal of Geophysical Research: Oceans* **118**, 1658–1672 (2013). URL https://doi.org/10.1002/jgrc.20122.